Title

Acceleration of tropical cyclogenesis by self-aggregation feedbacks

Authors

Muller, Caroline J
Romps, David M

Peer reviewed

Acceleration of tropical cyclogenesis by self-aggregation feedbacks

Caroline J. Muller[a,1] and David M. Romps[b,c]

[a]Laboratoire de Met´ eorologie Dynamique (LMD)/Institut Pierre Simon Laplace (IPSL), ´ Ecole Normale Sup ´ erieure, Paris Sciences & Lettres (PSL) Research ´ University, Sorbonne Universite,´ Ecole Polytechnique, CNRS, F-75005 Paris, France; ´ [b]Department of Earth and Planetary Science, University of California, Berkeley, CA 94720; and [c]Climate and Ecosystem Sciences Division, Lawrence Berkeley National Laboratory, Berkeley, CA 94720

1 To whom correspondence should be addressed. Email: carolinemuller123@gmail.com

Significance

Although the prediction of tropical cyclone tracks has improved in recent years, understanding the mechanisms responsible for the genesis and intensification of tropical cyclones remains a major scientific challenge. In this work we show that self-aggregation, a phenomenon discovered recently in idealized simulations of the tropical atmosphere, plays a leading-order role in the genesis of tropical cyclones in cloud-resolving simulations. This suggests that self-aggregation, and the framework developed for its study, could help shed more light into the physical processes leading to cyclogenesis and cyclone intensification. This work adds to the growing literature on the importance of this phenomenon for the tropical atmosphere.

Abstract

Idealized simulations of tropical moist convection have revealed that clouds can spontaneously clump together in a process called self-aggregation. This results in a state where a moist cloudy region with intense deep convection is surrounded by extremely dry subsiding air devoid of deep convection. Because of the idealized settings of the simulations where it was discovered, the relevance of self-aggregation to the real world is still debated. Here, we show that self-aggregation feedbacks play a leading-order role in the spontaneous genesis of tropical cyclones in cloud-resolving simulations. Those feedbacks accelerate the cyclogenesis process by a factor of 2, and the feedbacks contributing to the cyclone formation show qualitative and quantitative agreement with the self-aggregation process. Once the cyclone is formed, wind-induced surface heat exchange (WISHE) effects dominate, although we find that self-aggregation feedbacks have a small but nonnegligible contribution to the maintenance of the mature cyclone. Our results suggest that self-aggregation, and the framework developed for its study, can help shed more light into the physical processes leading to cyclogenesis and cyclone intensification. In particular, our results point out the importance of the longwave radiative cooling outside the cyclone.

Few geophysical phenomena are as spectacular as tropical cyclones (TCs). The cloud-free eye with weak motion is surrounded by an eyewall with clouds and rotating winds among the strongest on the planet. Although the prediction of cyclone tracks has improved in recent years, understanding the mechanisms responsible for the genesis and intensification of cyclones remains a major scientific challenge (1).

In the past decade or so, the increase in computational power permitted cloud-resolving models (CRMs) (with kilometer-scale resolution) to be run on large, mesoscale domains (hundreds of kilometers). Such simulations resolve the dynamics of clouds as well as their spatial organization at larger mesoscales. This led to the discovery of a remarkable tendency of convection to spontaneously aggregate in space at mesoscales. This phenomenon, called self-aggregation, was first discovered in idealized high-resolution cloud-resolving simulations of deep convection. Since then, self-aggregation has been found to be robust in numerous models, from CRMs where convection is resolved to full global climate models (GCMs) with parameterized convection, typically run in idealized settings, e.g., nonrotating doubly periodic radiative–convective equilibrium (RCE). Nonrotating RCE is an idealization of the tropical atmosphere in which the rotation of the earth is neglected, and the radiative cooling of the atmosphere is in equilibrium with the convective heating (2–4). Because of these idealized settings, the relevance of self-aggregation to our climate is still debated. Our goal is to see whether these newly discovered aggregating feedbacks in idealized cloud-resolving simulations play a role in cyclogenesis on a rotating planet.

Self-aggregation is strongly driven by longwave (LW) radiative feedbacks (5). More precisely, low-level radiative cooling in dry regions (due to clear sky and low-level clouds) and midlevel radiative warming in moist regions (due to high clouds) both contribute to the self-aggregation process (6). It is the resulting differential radiative cooling between dry and moist regions which is key, since it results in a low-level circulation that transports moist static energy (MSE) from dry, low-energy regions into moist high-energy regions (3, 6). This upgradient circulation reinforces the energy gradient, thereby strengthening the aggregation of convection.

As mentioned above, most studies of self-aggregation focused on idealized simulations, in particular RCE with no large-scale forcing and neglecting Earth's rotation. Neglecting Earth's rotation, i.e., setting $f = 0 \text{ s}^{-1}$ where f denotes the Coriolis parameter, is a reasonable approximation near the equator and at small scales, but becomes questionable when the convective aggregate reaches mesoscales. At those scales, the effect of Earth's rotation starts to be appreciable.

The present study addresses one aspect of these idealizations by investigating the impact of the background planetary rotation on self-aggregation and asking the following questions: Is self-aggregation relevant to the formation of TCs? Or are the feedbacks identified in idealized simulations not robust to planetary rotation? Are they dominated by other processes once rotation is accounted for?

Earlier studies of rotating RCE, sometimes referred to as a "tropical cyclone world," mainly investigated the properties of the mature cyclones [including the size and the distance between cyclones (7–10)]. Here, instead, we focus on the onset of cyclone formation, and our goal is to compare in detail cyclogenesis with the onset of convective self-aggregation. To that end, we perform a series of sensitivity runs where various feedbacks are turned on or off. More precisely, we focus on the relative role of the following two feedbacks: radiation feedbacks and surface–flux feedbacks. Radiation feedbacks include low-cloud, high-cloud, and clear-sky feedbacks, which have all been shown to contribute positively to self-aggregation (6). Surface–flux feedbacks connect enhanced surface winds to enhanced surface fluxes, and this connection, often referred to as a wind-induced surface heat exchange (WISHE) feedback, plays a key role in maintaining tropical cyclones (11).

Our work builds upon the recent work of refs. 8 and 10, which investigates the spontaneous generation of tropical cyclones from homogeneous conditions in rotating radiative–convective equilibrium. In particular, ref. 10 suggests that radiative feedbacks, known to be key for self-aggregation, could accelerate cyclogenesis, a result that we further investigate and quantify here.

Results

Fig. 1 shows snapshots from a control (CTRL) simulation and three sensitivity simulations: CTRL (Fig. 1A) with all feedbacks turned on [radiation (RAD) feedbacks and surface-flux (SFC) feedbacks, see *Materials and Methods* for details]; noSFC-noRAD (Fig. 1B) with all feedbacks turned off; noRAD (Fig. 1C) with interactive radiation turned off; and noSFC (Fig. 1D), where feedbacks associated with interactive surface fluxes are turned off (in particular WISHE effects are off). The variable shown is the vertically integrated moist static energy

$$\int \mathrm{MSE} = \int_0^{z_t} (c_p\,T + gz + L_v\,q_v)\,\rho\,dz, \qquad [1]$$

where z_t is the tropopause height, c_p the specific heat of air, T the temperature, g gravity, L_v the latent heat of vaporization, q_v the water vapor mixing ratio, and ρ density. $\int$MSE is a useful variable since it is conserved during moist adiabatic processes in this model (neglecting subgrid-scale fluxes and latent heat contributions from the ice phase). Hence its mass-weighted vertical integral can be changed only by radiation, surface fluxes,

and advection. In the tropics, where horizontal temperature gradients are small, its variability is closely related to that of water vapor. Consistently, snapshots of precipitable water $\int_0^{z_t} q_v \; \rho \; dz$ show a very similar spatial distribution to that of ∫MSE, the only difference being that the eye of the cyclone is visible in precipitable water (dry anomaly), while it is not seen in ∫MSE since the dryness in the eye is largely compensated by warmer conditions due to adiabatic compression. Also shown is the time evolution of the SD of ∫MSE and of the domain-mean wind speed near the surface (first atmospheric level at 37.5 m, Fig. 1 *E–H*), both indicative of the TC intensification. Convective organization in general is associated with an increase in ∫MSE variance, as moist regions become moister and dry regions become drier (12, 13).
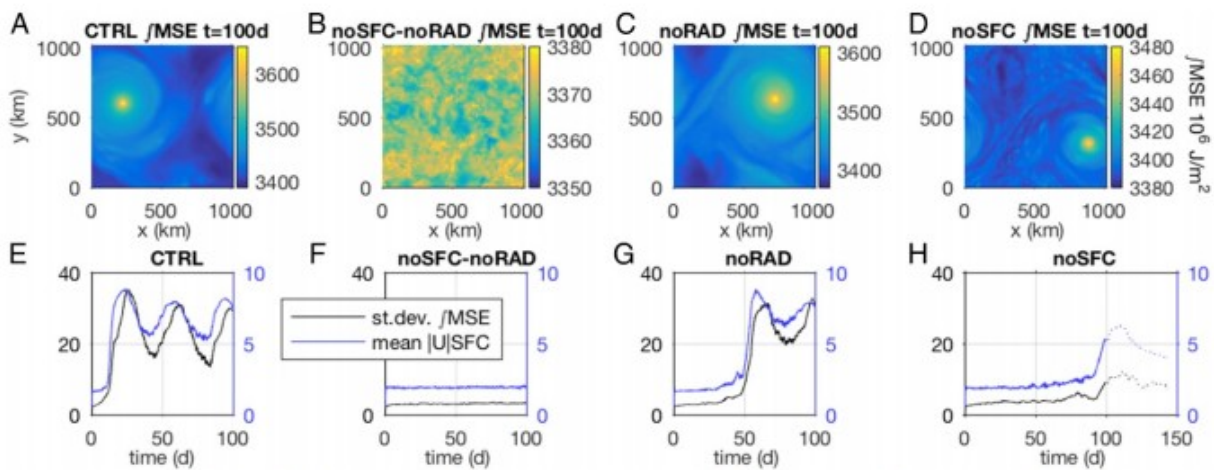

Fig. 1. Cyclone evolution in CTRL and sensitivity runs. (*A–D*) Snapshots of ∫MSE at day 100 of the simulations. (*E–H*) Time evolution of the SD of ∫MSE and of the domain-averaged wind speed near the surface (m·s^{-1} at the first atmospheric level $z = 37.5$ m).

The CTRL run develops a cyclone in about 25–30 d, with a minimum surface pressure of about 930 hPa. When all feedbacks are turned off (noSFC-noRAD), no cyclone develops, as expected, since interactive surface fluxes are believed to be key for TCs (this remains true if we run it longer; no cyclone develops even after 250 d of simulation). Surprisingly, though, if only radiative feedbacks are removed (noRAD), the cyclogenesis takes about 60 d, which is more than twice as long as in the CTRL run. This suggests that aggregation feedbacks accelerate the cyclogenesis process (at least in the absence of large-scale forcing) by a factor of about 2. Perhaps even more surprisingly, if just surface–flux feedbacks are removed (noSFC), the simulation still yields a weak "radiative cyclone." In other words, radiative feedbacks are sufficient to yield a cyclone, even without interactive surface fluxes (i.e., even without WISHE). The TC is still intensifying after 100 d of simulations, but remains weaker than in CTRL even if we run them longer (Fig. 1*H*). Without the wind-induced enhancement of turbulent surface fluxes, the TC cannot reach its full intensity in the mature stage. However, the fact

that radiative feedbacks on their own are sufficient to initiate even a weak cyclone is remarkable.

Also note that, once the TC is formed, whether radiative feedbacks are turned on or not, the cyclone intensity is to leading order the same, although there is a slight reduction without interactive radiation (7% reduction between CTRL and noRAD of the high percentiles of the SD of ∫MSE and 15% reduction of the high percentiles of surface wind speed; similar reductions, between 5% and 15%, are found based on high percentiles of precipitable water and latent heat flux). This is again consistent with our current understanding of TCs, whose main sources of energy in the mature stage are interactive surface fluxes (14). But we find here that the radiative feedbacks are responsible for a small but nonnegligible contribution to the intensity of the mature cyclone, consistent with an earlier study pointing out the importance of radiation in the maintenance of a cyclone intensity (10). Before moving on, it is interesting to note that the mature cyclone undergoes three periods of intensification in CTRL. A similar variability was noted in ref. 10. We hypothesize that these periods are related to a vertical wind shear which develops as the TC strengthens (Fig. S1).

Role of Radiative Feedbacks in Timing of Cyclone Formation

Let us now investigate further the impact of radiative feedbacks on the time needed to reach a fully developed cyclone. Both cyclogenesis and self-aggregation have been shown to be sensitive to initial conditions (10, 15). We verify that the slowdown of cyclone formation without radiative feedbacks is robust to initial conditions (Fig. 2*A*), with a factor of 2 or larger for all initial conditions. In fact, for all of the initial conditions tried here, the control simulation was faster than any sensitivity simulation (noRAD, noSFC, or noSFC-noRAD) that we tried (Fig. S2). Also, separately removing the shortwave (SW) and LW contributions to the radiation highlights the key role of LW radiative feedbacks (Fig. 2*B*): Removing the interactive SW radiation has little impact, while removing the interactive LW radiation slows down the cyclone formation even more than noRAD. This suggests a similarity with the nonrotating self-aggregation process for which LW feedbacks are known to be crucial. Also consistent with self-aggregation is the fact that the three terms in the LW radiative cooling, LW cooling from liquid clouds, ice clouds, and clear sky, all contribute positively to the acceleration of the cyclogenesis process (Fig. 2*C*). Indeed, removing each separately does not account for the overall slowdown of the cyclogenesis.
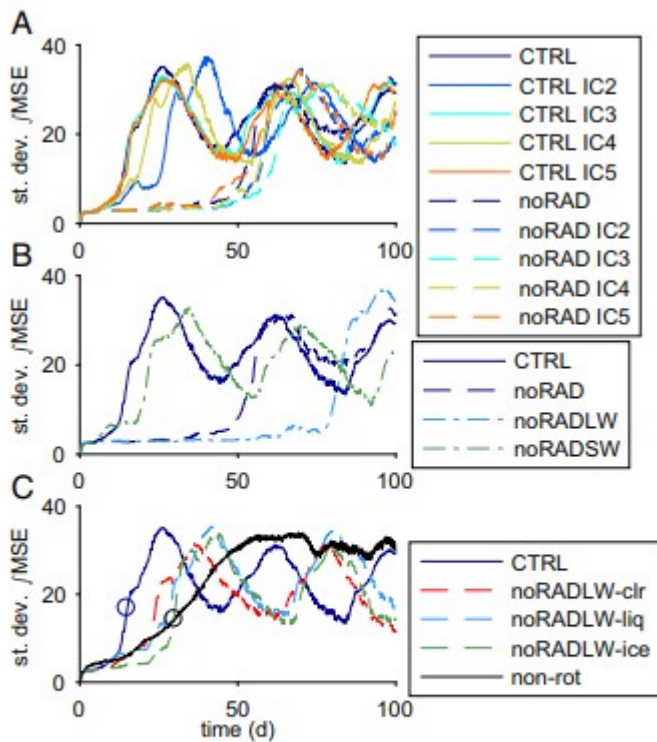
Fig. 2. Time evolution of the SD of ∫MSE (10^6 J·m^{-2}) (*A*) for different initial conditions; (*B*) in sensitivity runs removing separately the SW and LW interactive radiation; and (*C*) in sensitivity runs removing the LW liquid cloud, ice cloud, and clear-sky contributions separately. Open circles in *C* indicate the first 15 d of cyclogenesis and the first 30 d of nonrotating self-aggregation.

These results are qualitatively consistent with those of ref. 10 (their figure 4), which also finds that removing radiative feedbacks delays cyclogenesis. To further quantify the impact of radiative feedbacks on the timescale of convective organization, we perform a larger ensemble of CTRL and noRAD simulations (Fig. S3). We find that the acceleration of cyclogenesis by radiative feedbacks is extremely robust. Interestingly, the variability of the timescale of convective organization is smaller in our CTRL simulations than in ref. 10. We hypothesize that this is due to the different radiation scheme used [Rapid Radiative Transfer Model (RRTM) vs. National Center for Atmospheric Research (NCAR) Community Atmosphere Model (CAM) here], since ref. 10's simulations without radiative feedbacks yield a smaller variability. Other differences in our settings could also play a role (in particular, they use a warmer sea-surface temperature of 305 K compared with 300 K here).

Fig. 3 further shows similarities between self-aggregation and cyclogenesis. It shows the radiative cooling rates and streamfunctions (see *Materials and Methods* for details about the computation), as well as cloud content, in the cyclone (Fig. 3*A*) and self-aggregation (Fig. 3*B*) runs, as a function of height and rank of vertically integrated ∫MSE. We focus on the genesis, and hence

we show days 1–15 for the cyclone (blue open circle in Fig. 2*C*; day 15 is about halfway to the full cyclone) and days 1–30 for self-aggregation (black open circle in Fig. 2*C*, where similarly day 30 is about halfway to the full aggregation). The self-aggregation plot is slightly less noisy since it contains more days. In both cases, though, there is strong low-level radiative cooling in dry regions (strong cooling between the surface and 2 km in the dry columns below rank 20) from clear sky and low-level liquid clouds, which promotes aggregation (6). We also see the midlevel radiative warming in moist convective regions from middle and high clouds (warming in the moistest columns above 5 km) also known to enhance aggregation (6).
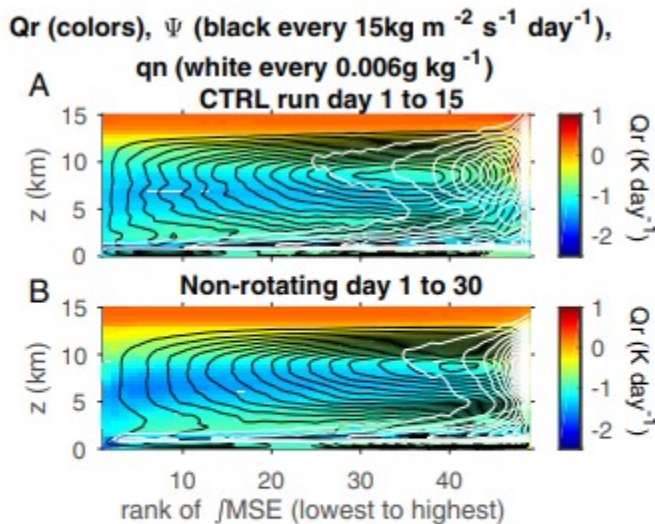
Fig. 3. Cyclogenesis vs. self-aggregation. (*A* and *B*) Circulation between dry and moist columns during (*A*) the formation of the tropical cyclone in CTRL and (*B*) the onset of self-aggregation in a nonrotating simulation. The dry columns are on the left (low ∫MSE rank), and the moist columns are on the right (high rank). Plain black contours indicate counterclockwise circulation, and white contours indicate cloud condensates.

We can compare the circulation with the one expected from radiative cooling rates only, assuming that radiative cooling is exactly balanced by subsidence warming. This is expected to be true outside of clouds (in cloudy regions, however, the latent heat also enters the temperature equation and therefore contributes to vertical velocities). Consistently, there is a good agreement in the dry regions away from clouds between the circulation expected from radiative cooling rates only and the actual circulation (Fig. S4). The differential radiative cooling between dry and moist regions is therefore largely responsible for the low-level subsidence seen in Fig. 3 below 2 km in the driest columns (up to rank 10 or so). This subsidence is accompanied by a flow from dry to moist columns near the surface (up to rank 20), rising above 2 km in the moister columns (rank 20 or higher). This low-level circulation from dry to moist regions is crucial since it transports MSE upgradient, from dry to moist regions, favoring aggregation (3, 5, 6). These results suggest a close similarity between cyclogenesis and the idealized self-aggregation process. Let us now quantify this in more detail.

Comparison with Nonrotating Self-Aggregation

We compare quantitatively the process of self-aggregation and cyclogenesis by investigating the precise contribution of each feedback to the convective organization. We use a framework (12) based on the $\int$MSE variance time evolution. As noted earlier, $\int$MSE can only be changed by radiation, surface fluxes, and advection to leading order. Convective organization is characterized by larger $\int$MSE variance than disorganized convection. The equation for the time evolution of the variance of $\int$MSE can therefore be used to quantify the contribution from each feedback to the increase of the variance accompanying convective organization (for both aggregation and cyclogenesis). This equation is

$$\frac{1}{2}\frac{d\left(\int \text{MSE}'\right)^2}{dt} = \int \text{MSE}'\ \text{SFC}' + \int \text{MSE}'\ \text{LW}' + \int \text{MSE}'\ \text{SW}'$$
$$+ \int \text{MSE}'\ C'_{\text{MSE}}, \qquad\qquad [2]$$

where a prime denotes departure from the domain mean, SFC denotes surface fluxes (latent and sensible), LW is longwave net heating rate of the atmosphere (LW_{SFC}-LW_{TOA}, where TOA refers to top-of-atmosphere), SW is shortwave net heating rate of the atmosphere (SW_{TOA}-SW_{SFC}), and C_{MSE} is the horizontal convergence of MSE flux vertically integrated. Positive contributions imply positive feedbacks. For instance, if surface fluxes are anomalously positive ($\text{SFC}' > 0$) in the high-$\int$MSE region ($\int$MSE $' > 0$), surface fluxes increase energy in the high-energy region, thereby strengthening the gradient, yielding a positive feedback. This equation allows a quantitative comparison of direct diabatic feedbacks between nonrotating self-aggregation and cyclogenesis (we call them direct diabatic feedbacks as they do not account for the circulation, hence energy transport, associated with cooling/warming from the diabatic terms). Fig. 4 shows the $\int$MSE variance contributions in the self-aggregation process and during cyclogenesis. Fig. 4 *A* and *F* shows the domain mean feedback contributions, while Fig. 4 *B–E* and *G–J* shows contributions as a function of rank of $\int$MSE (dry columns on the left, moist columns on the right).
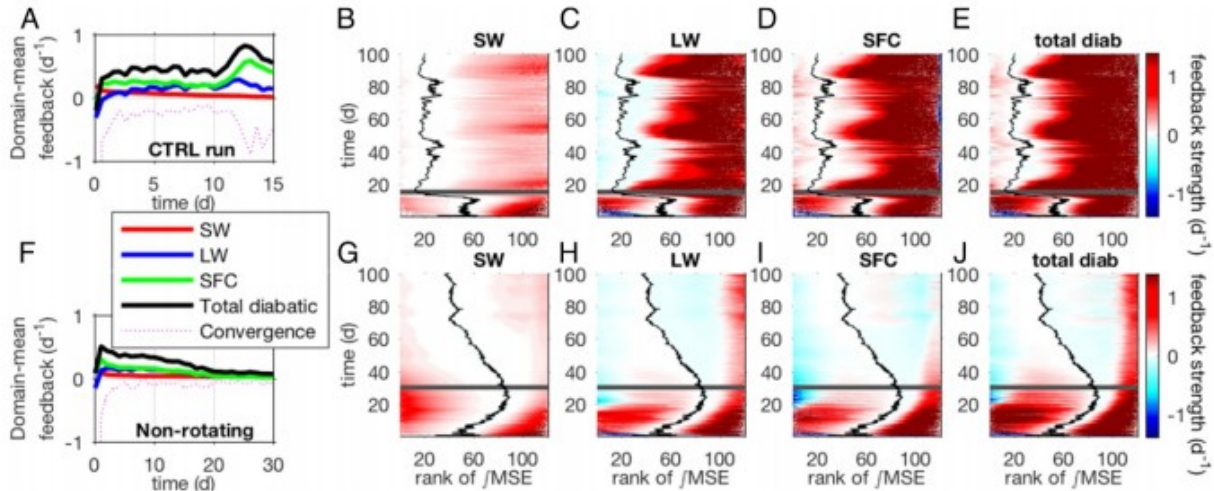
Fig. 4. Strength of feedbacks leading to convective organization estimated from Eq. 2 (normalized by the variance of ∫MSE and thus in d⁻¹). The feedback contributions to cyclogenesis (CTRL, *A–E*) and to the onset of self-aggregation (nonrotating, *F–J*) are shown. The domain mean contributions are shown in *A* and *F*, while detailed contributions in dry (low ∫MSE) and moist (high ∫MSE) regions are shown (*B–E* and *G–J*). The black curves indicate zero ∫MSE anomaly, and thus dry regions lie to their left while moist regions lie to their right. The gray line indicates day 15 of the cyclogenesis and day 30 of the self-aggregation. Note that the color bars in *C–J* are saturated as in earlier studies (10, 12), to ease comparison.

The genesis of the tropical cyclone resembles an accelerated nonrotating self-aggregation. Specifically Fig. 4 shows that the first 15 d of cyclogenesis resemble the first 30 d of aggregation (gray lines in the feedback contour plots in Fig. 4 *B–E* and *G–J*, which are also shown as open circles in Fig. 2*C*). Indeed, up to about halfway to the full cyclone/aggregation, the feedback strengths and distributions (as a function of rank of ∫MSE) are very similar between the rotating and nonrotating simulations. They diverge about halfway to the full TC/aggregation when surface feedbacks become different: positive for the cyclone, while weak and slightly negative for aggregation (Fig. 4 *D* and *I*).

Although the leading-order feedback, once the cyclone is formed, comes from interactive surface fluxes, the contribution from high-cloud LW radiation is significant, about one-third to one-half that of the surface (Fig. 4*A*). This is consistent with an earlier study (10), which finds that radiative feedbacks contribute to half the ∫MSE variance in a mature cyclone. So the picture that emerges is the following: Self-aggregating feedbacks can strongly accelerate cyclogenesis. In fact, radiative feedbacks alone are sufficient to yield a weak radiative cyclone. Once the mature cyclone is formed though, interactive surface fluxes are the main source of energy and dictate its intensity to leading order, with a small but nonnegligible contribution from high-cloud radiative feedbacks.

Although our main focus is on the genesis process, we think that the radiative cyclone in Fig. 1*D* is intriguing and deserves further discussion. In particular, an interesting question is whether convection in the radiative cyclone is similar to convection in the control cyclone (Fig. 1*A*) or whether it resembles regular disorganized "popcorn" convection (Fig. 1*B*). A useful diagnostic to characterize the convection is the circulation in thermodynamic

variables, more precisely the streamfunction as a function of two variables: height and pointwise MSE (not the vertically integrated ∫MSE discussed above) (16, 17).

Let us start with CTRL. Fig. 5*A* shows three MSE surfaces, the highest MSE corresponding to air ascending in the wall near the eye of the tropical cyclone, while lower MSE surfaces are found farther away from the eye. Fig. 5*B* shows the circulation as a function of MSE and height. Compared to regular popcorn disorganized convection (Fig. 5*D*), the updrafts at high MSE in CTRL show less entrainment, as can be seen by the more vertical contours at high MSE ($\approx\approx$350 K) in Fig. 5*B*. In other words, MSE is more constant in updrafts in CTRL than in disorganized convection, where entrainment of environmental lower MSE air decreases MSE during the ascent in Fig. 5*D*.
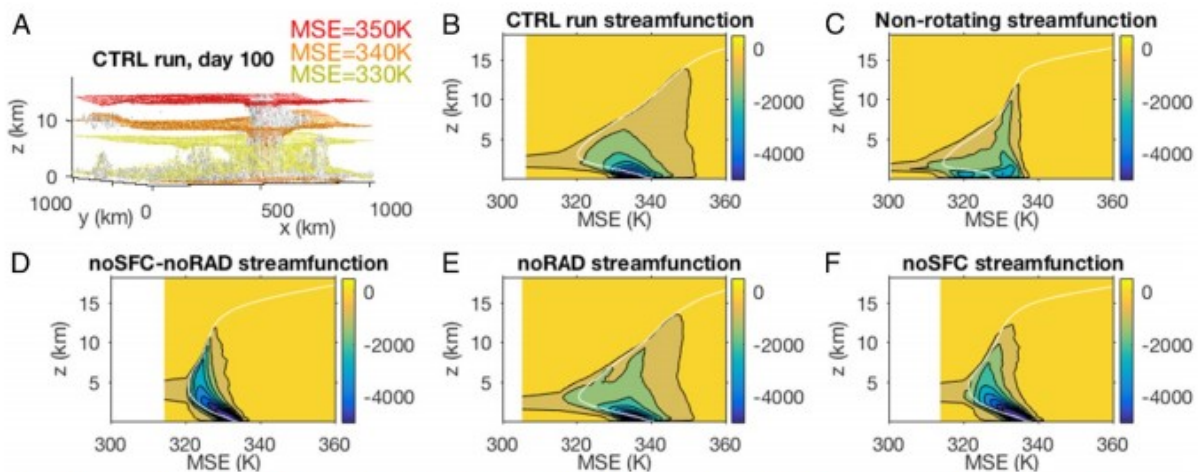

Fig. 5. Streamfunction vs. MSE and height. Shown is circulation (kg·m^{-2}·s^{-1}) in thermodynamic coordinates MSE and height in (*B*) CTRL and (*C*–*F*) nonrotating and sensitivity runs averaged between day 95 and day 100. *A* illustrates three MSE surfaces in CTRL. The white lines indicate the domain-mean MSE. Black contours are shown every 700 kg·m^{-2}·s^{-1}.

At moderate MSE, the MSE is reduced as the air ascends in updrafts in both CTRL and noSFC-noRAD, due to entrainment of ambient lower MSE air. The MSE decreases during descent due to radiative cooling, until surface fluxes make the MSE increase again near the surface (below 2 km). The cyclone yields large mean MSE and large MSE variability compared with regular popcorn disorganized convection. The large enhancement of MSE variability with convective organization is consistent with Fig. 1.

The cyclone without radiative feedbacks (Fig. 5*E*) is very similar to the control cyclone. Note also the similarity with the nonrotating self-aggregation (Fig. 5*C*), which exhibits large MSE variability and little entrainment in updrafts. This is consistent with the fact that, in all organized cases, the spatial organization of convection isolates updrafts from drier environmental air, reducing the entrainment. But self-aggregation leads to much drier conditions, and hence much lower mean MSE, compared with a cyclone.

Interestingly, the radiative cyclone (Fig. 5*F*) lies somewhere between the disorganized convection (Fig. 5*D*) and the tropical cyclone (Fig. 5*A*), with intermediate MSE variability, but is overall closer to disorganized convection. This is consistent with our earlier results that, to leading order, the mature cyclone is fed by interactive surface fluxes. The radiative cyclone is therefore expected to be weak.

Summary and Discussion

The overall picture that emerges is that the feedbacks identified in idealized settings as leading to the spontaneous self-aggregation of convection play an important role in cyclogenesis. More precisely, the onset of self-aggregation in nonrotating simulations shares qualitative and quantitative properties with tropical cyclogenesis. Radiative feedbacks are found to accelerate the cyclogenesis by a factor of 2 or larger. The LW radiative feedback is the key contribution to those radiative feedbacks, as in self-aggregation. Surprisingly, radiative feedbacks by themselves are sufficient to yield a cyclone, albeit weak, even in the absence of WISHE effects.

The early times of cyclogenesis in the CTRL simulation resemble accelerated self-aggregation (days 1–15 for the TC and days 1–30 for the self-aggregation), with similar contributions from the various feedbacks to the development of organized convection. The simulations then diverge when interactive surface fluxes become a strong positive feedback in CTRL, due to strong winds and surface fluxes in the flow converging into the cyclone, while they become a small negative feedback in the self-aggregation, due to strong surface latent fluxes in the dry subsidence region, consistent with ref. 10.

We acknowledge that the simulations used in this study are still idealized, e.g., doubly periodic and in RCE, without large-scale forcing. In the real tropics, the route to tropical cyclogenesis can be quite different and is influenced by large-scale environmental conditions, such as the passing of an equatorial wave and preexisting favorable moist conditions within a "marsupial pouch" (18). Comparison of the timescale of self-aggregation tendencies investigated here to that of large-scale environmental conditions deserves further investigation using more realistic simulations. Our results suggest that self-aggregation, and the framework developed for its study, can help shed more light on the physical processes leading to cyclogenesis and cyclone intensification. In particular, our results point out the importance of the LW radiative cooling at low levels outside the cyclone and the low-level circulation that it entails. Further comparison with data and analysis of simulations in more realistic settings are desirable to clarify the precise contribution and location of the LW radiative feedback.

Materials and Methods

The CRM used in this study is the System for Atmospheric Modeling (SAM) (19). All of the runs are in doubly periodic geometry starting from

homogeneous initial conditions and with an imposed sea-surface temperature of 300 K. The resolution is 4 km and the domain size 1,024 km in both horizontal directions. The vertical grid has 64 levels with the first level at 37.5 m and grid spacing gradually increasing from 80 m near the surface to 400 m above 5 km. To reduce gravity wave reflection and buildup, Newtonian damping is applied to all prognostic variables in the upper third of the model domain. Given the large number of sensitivity simulations needed for this study, we reduce the computational cost by using a value of the Coriolis parameter $f = 10^{-4} \text{ s}^{-1}$, larger than typical tropical values; this reduces the size of TCs (7), allowing simulated TCs to fit in our 1,024 × 1,024 km² domain. The sensitivity simulations are all based on CTRL with the following perturbations: noSFC, surface fluxes homogenized horizontally at each time step; noRAD, radiative cooling homogenized horizontally at each time step and height; noRADSW (resp. noRADLW), SW (resp. LW) radiative cooling homogenized horizontally at each time step and height; noRADLW-clr, homogenize at each time step and height the temperature and water vapor entering the LW radiative cooling; noRADLW-liq (resp. noRADLW-ice), contribution from cloud liquid (resp. cloud ice) water to LW radiative cooling zeroed; nonrotating, $f = 0 \text{ s}^{-1}$. The streamfunction in Fig. 3 and Fig. S4 is given by ref. 3: $\Psi_{i+1}(z) = \Psi_i(z) + (\rho w)_i(z)$, where $(\rho w)_i$ is the total mass flux contribution from the ith rank of ∫MSE.

References

1. De Maria M, Sampson CR, Knaff JA, Musgrave KD (2014) Is tropical cyclone intensity guidance improving? Bull Am Meteorol Soc 95:387–398.

2. Held IM, Hemler RS, Ramaswamy V (1993) Radiative-convective equilibrium with explicitly two-dimensional moist convection. J Atmos Sci 50:3909–3927.

3. Bretherton CS, Blossey PN, Khairoutdinov M (2005) An energy-balance analysis of deep convective self-aggregation above uniform SST. J Atmos Sci 62:4237–4292.

4. Wing AA, Emanuel K, Holloway CE, Muller C (2017) Convective self-aggregation in numerical simulations: A review. Surv Geophys 38:1173–1197.

5. Muller CJ, Held IM (2012) Detailed investigation of the self-aggregation of convection in cloud-resolving simulations. J Atmos Sci 69:2551–2565.

6. Muller CJ, Bony S (2015) What favors convective aggregation and why? Geophys Res Lett 42:5626–5634.

7. Khairoutdinov M, Emanuel K (2013) Rotating radiative-convective equilibrium simulated by a cloud-resolving model. J Adv Model Earth Syst 5:816–825.

8. Davis CA (2015) The formation of moist vortices and tropical cyclones in idealized simulations. J Atmos Sci 72:3499–3516.

9. Shi X, Bretherton CS (2014) Large-scale character of an atmosphere in rotating radiative-convective equilibrium. J Adv Model Earth Syst 6:616–629.

10. Wing AA, Camargo SJ, Sobel AH (2016) Role of radiative-convective feed-backs in spontaneous tropical cyclogenesis in idealized numerical simulations. J Atmos Sci 73:2633–2642.

11. Emanuel KA (1986) An air sea interaction theory for tropical cyclones. Part I: Steadystate maintenance. J Atmos Sci 43:585–604.

12. Wing AA, Emanuel KA (2014) Physical mechanisms controlling self-aggregation of convection in idealized numerical modeling simulations. J Adv Model Earth Syst 6:59–74.

13. Wing AA, Cronin TW (2016) Self-aggregation of convection in long channel geometry. Q J R Meteorol Soc 142:1–15.

14. Emanuel K (2003) Tropical cyclones. Annu Rev Earth Planet Sci 31:75–104.

15. Khairoutdinov M, Emanuel K (2010) Aggregated convection and the regulation of tropical climate. 29th Conference on Hurricanes and Tropical Meteorology, Extended Abstracts, p P2.69.

16. Pauluis OM, Mrowiec AA (2013) Isentropic analysis of convective motions. J Atmos Sci 70:3673–3688.

17. Mrowiec AA, Pauluis OM, Zhang F (2016) Isentropic analysis of a simulated hurricane. J Atmos Sci 73:1857–1870.

18. Dunkerton TJ, Montgomery MT, Wang Z (2009) Tropical cyclogenesis in a tropical wave critical layer: Easterly waves. Atmos Chem Phys 9:5587–5646.

19. Khairoutdinov MF, Randall DA (2003) Cloud resolving modeling of the ARM summer 1997 IOP: Model formulation, results, uncertainties, and sensitivities. J Atmos Sci 60:607–625.